

## Analysis of the Thermally Induced Structural Changes of Bovine Lactoferrin

Nicoleta Stănciuc,<sup>†</sup> Iuliana Aprodu,<sup>\*,†</sup> Gabriela Râpeanu,<sup>†</sup> Iesel van der Plancken,<sup>‡</sup> Gabriela Bahrim,<sup>†</sup> and Marc Hendrickx<sup>‡</sup>

<sup>†</sup>Faculty of Food Science and Engineering, “Dunarea de Jos” University of Galati, 111 Domneasca Street, 800201, Galati, Romania

<sup>‡</sup>Laboratory of Food Technology, Leuven Food Science and Nutrition Research Center (LForCe), Katholieke Universiteit Leuven, Kasteelpark Arenberg 22, B3001 Heverlee, Belgium

**ABSTRACT:** Bovine lactoferrin (LF) is subjected to thermal processing during isolation for commercial use and while preparing milk products intended for infant nutrition. The present study is focused on the heat-induced structural changes of LF in buffer solution. Fluorescence spectroscopy, molecular modeling, and enzymatic hydrolysis studies were combined to extensively characterize LF thermal behavior. The temperature-induced changes induced on LF conformation were analyzed through intrinsic and ANS fluorescence parameters (intensity, maximum position, and parameter *A* value), the phase diagram method, and quenching experiments using acrylamide and iodide. A higher exposure of hydrophobic residues was highlighted through the molecular modeling approach, with a decrease in  $\alpha$ -helix content from 23.5% to 21.2% when increasing the temperature from 25 °C to 80 °C. The experimental results demonstrate a more flexible conformation of the protein at higher temperature, thus facilitating the enzymatic hydrolysis by thermolysin.

**KEYWORDS:** lactoferrin, conformational changes, fluorescence spectroscopy, molecular modeling, enzymatic hydrolysis

### INTRODUCTION

Lactoferrin (LF) is an active natural glycoprotein-combined protein with significant physiological functions such as immunoregulation and cell proliferation.<sup>1</sup> LFs are single-chain polypeptides of about 80 kDa containing one to four glycans, depending on the species.<sup>2</sup> LF is an iron-binding protein that belongs to the transferrin group of proteins and binds two high-spin Fe<sup>3+</sup> ions with very high affinity.<sup>3</sup> LF may be found in both iron-saturated (holo-) and iron-depleted (apo-) forms.

Bovine LF consists of 689 amino acids, and the protein is bilobal. Each lobe consists of two domains and a single, high-affinity metal binding site, which binds, very tightly but reversibly, one ferric ion together with one carbonate as the synergistic anion. Each iron-binding site consists of the same set of six ligating groups: the phenolic oxygens of two Tyr residues, the imidazole group of a His residue, the carboxylate group of an aspartic acid residue, and two oxygens of the bidentate carbonate synergistic anion. The two sites are too distant (35 nm) for direct interaction between them.<sup>4</sup>

In bovine LF there are five potential sites for N-bound glycan structures, given by Asn residues at positions 233, 281, 368, 476, and 545. The chemical analysis, however, reveals only four N-linked glycans; apparently Asn<sup>281</sup> is not used.<sup>5</sup> LF has a relatively high pI (8–9), which can be explained by a unique alkaline region in the N terminal region, which can bind acidic molecules.<sup>6</sup>

Although present in milk as a result of *in situ* synthesis within the mammary gland, it is also present in several other exocrine fluids. Apo-LF has a bactericidal effect against a wide range of microorganisms: Gram-positive and Gram-negative bacteria as well as yeasts. Some peptides generated through LF hydrolysis, such as lactoferricin<sup>7</sup> and lactoferrampin,<sup>8</sup> have been shown to exhibit microbicidal activity. In addition, LF may play important

roles in intestinal iron uptake and regulation, immune response, growth factor activity, bone growth, and antioxidant activity.<sup>9</sup> Bovine LF has been used in a wide variety of products such as infant formulas, probiotics, supplemental tablets, pet food, and cosmetics and as a natural solubilizer of iron in food.<sup>10</sup>

There are few reports available on the heat-induced structural and conformational changes of LF. Abe et al. (1991)<sup>11</sup> and Sreedhara et al. (2010)<sup>12</sup> suggested a stable conformation at acidic and neutral pH. Polverino de Lauro et al. (1999)<sup>13</sup> have shown that limited proteolysis experiments are useful for probing protein structure and dynamics, thus complementing the results that can be obtained by using other common physicochemical methods and approaches.

In order to get a comprehensive evaluation of complex molecular systems, computational and experimental approaches can be successfully combined, although are frequently considered as competing resources.<sup>14,15</sup> Molecular modeling techniques are effective investigative tools for complementing experiments and theoretical models.<sup>14</sup> In particular molecular dynamics simulations can be successfully used for adding detailed information at the atomic level on the biomolecules' behavior. On the other hand, the structure and dynamics of protein molecules in solution, such as heat-induced behavior, can be investigated through fluorescence due to the sensitivity of intrinsic fluorescence of Trp residues to their microenvironments.<sup>16</sup>

The aim of this work was to compare the heat-induced changes in commercial LF conformation and structure in the

**Received:** August 21, 2012

**Revised:** February 13, 2013

**Accepted:** February 14, 2013

**Published:** February 14, 2013

temperature range of 60 to 80 °C using different approaches. Fluorescence spectroscopic measurements (tryptophan fluorescence, ANS-binding, acrylamide, and KI quenching experiments, phase diagram) were employed for a comprehensive characterization of heat-induced structural changes of LF. Further insight into the determinants of structural changes of LF during thermal treatment was provided by means of molecular modeling tools. In addition, the susceptibility of LF to enzymatic hydrolysis using thermolysin was analyzed to better enlighten the extent of the thermally induced conformational changes.

## MATERIALS AND METHODS

**Materials.** Iron-saturated lactoferrin from bovine milk (approximately 90% purity by SDS gel electrophoresis, molecular weight ~87 kDa), 1-anilino-8-naphthalenesulfonate (ANS), (4-(2-hydroxyethyl)-1-piperazineethanesulfonic acid (HEPES), and acrylamide were obtained from Sigma (Sigma-Aldrich Co, St. Louis, MO, USA). The protein was used without further purification. All other chemicals used were of analytical grade.

**Heat Treatment.** The protein was dispersed in 10 mM Tris-HCl buffer (pH 7.2) to get a final concentration of 0.15 mg mL<sup>-1</sup>. The mixture was stirred at room temperature for 15 min. The protein solutions (0.075 mL) were filled in plastic tubes (1 cm diameter). The thermal treatment experiments were conducted in a thermostatic water bath at temperatures ranging from 60 to 80 °C for 10 min. The total time of the thermal treatment was long enough to ensure the structural rearrangements within the protein molecule, taking into account the low protein concentration used in the experiment. After the thermal treatment, the tubes were immediately cooled in ice water to prevent further denaturation. All measurements were performed within 3 min after the heat treatment. All spectroscopic studies were carried out on the heated-cooled protein, implying that only irreversible/permanent structural changes were detected. Before fluorescence spectroscopy analysis, the un-heat-treated protein solutions were diluted in buffer to a corresponding protein concentration of 0.001 mg mL<sup>-1</sup>.

**Fluorescence Spectroscopy Analysis. Intrinsic Fluorescence.** Intrinsic fluorescence measurements were made on a LS-55 luminescence spectrometer (PerkinElmer Life Sciences, Shelton, CT, USA) with a quartz cell of 10 mm path length, using an excitation wavelength of 292 nm. The emission was collected between 300 and 400 nm. The slits were 5 nm at excitation and 2.5 nm at emission, and the scan speed was 500 nm·min<sup>-1</sup>. Measurements were made at 25 °C. The position and form of the fluorescence spectra were characterized also by the parameter  $A [(I_{320}/I_{365})_{292}]$ , where  $I_{320}$  and  $I_{365}$  are fluorescence intensities at a  $\lambda_{em}$  of 320 and 365 nm, respectively, considering a  $\lambda_{ex}$  of 292 nm.<sup>17</sup>

**ANS Binding Measurements.** In order to study the binding of the hydrophobic dye ANS, the untreated protein samples were incubated for 15 min at 25 °C in the dark with 10  $\mu$ L of 8 mM ANS in 10 mM Tris-HCl buffer (pH 7.0). The fluorescence of ANS was excited at 365 nm, and emission was collected between 400 and 600 nm at 25 °C. Assays in the absence of the protein were performed in order to correct for unbound ANS emission fluorescence intensities.

**Phase Diagram Method.** As reported by Kuznetsova et al. (2004),<sup>18</sup> the phase diagram method is a sensitive approach for the detection of unfolding/refolding intermediates of proteins. The essence of the parametric dependencies method is to build up the diagram of  $I(\lambda_1)$  versus  $I(\lambda_2)$ , where  $I(\lambda_1)$  and  $I(\lambda_2)$  are the spectral intensity values measured at  $\lambda_1$  and  $\lambda_2$  under the different experimental conditions for a protein undergoing structural transformations. In principle,  $\lambda_1$  and  $\lambda_2$  are arbitrary wavelengths of the spectrum, but in practice such diagrams will be more informative if  $\lambda_1$  and  $\lambda_2$  will be on different slopes of the spectrum such as 320 and 365 nm for the fluorescence spectrum.

**Fluorescence Quenching Experiments.** Fluorescent quenching experiments were performed with acrylamide and KI. Acrylamide (8 M) and KI (5 M) were prepared freshly in 10 mM Tris-HCl buffer at

pH 7.0. Quenching titrations were performed by sequentially adding aliquots of the quencher stock solutions to the denatured samples followed by gently stirring. The excitation wavelength was set to 292 nm, and the fluorescence emission spectra were scanned from 300 to 400 nm.

The fluorescence quenching data were analyzed by fitting to the Stern–Volmer equation (eq 1):

$$\frac{F_0}{F} = 1 + K_{SV}[Q] \quad (1)$$

where  $F_0$  and  $F$  are the fluorescence intensities in the absence and presence of quencher,  $[Q]$  is the concentration of the quenchers, and  $K_{SV}$  is Stern–Volmer quenching constant.

**Molecular Modeling.** The molecular dynamics simulations were designed to estimate all reversible and irreversible conformational changes in the lactoferrin molecule induced by the thermal treatment. The X-ray crystallographic model of bovine LF<sup>19</sup> was obtained from the Brookhaven Protein Data Bank (code 1BLF.pdb). After the preliminary refinement of the molecular model consisting of the removal of water molecules, energy minimizations and molecular dynamics (MD) simulations were performed using the software Gromacs (version 4.5.5.).

The simulations were carried out in parallelization conditions on a Intel Core 2 CPU 6300 1.86 GHz processor-based machine running Linux using the Gromos96 43a1 force field.

The protein model was first minimized under vacuum using a sequence of two algorithms (steepest descent and limited-memory Broyden–Fletcher–Goldfarb–Shanno) to eliminate any strongly repulsive nonbonded contacts or geometric distortions.

The minimized structure was afterward placed in a rectangular box (119.46 Å × 119.46 Å × 119.46 Å) and was solvated by adding single point charge (SPC) explicit water molecules to model the protein–water interactions. The system consisting of 70 610 atoms (including 53 394 water molecules) was further prepared for MD steps by performing an additional energy minimization, using the above-mentioned procedure with the two algorithms in sequence.

To understand the atomic details of the thermally induced conformation changes on the LF molecule, different MD steps were performed to gradually increase the temperature to 25 and 80 °C by coupling each component of the system to a Berendsen thermostat for 100 ps. In order to remove any potential temperature and energy oscillations, the systems were further equilibrated for 1 ns. The time step used in all MD simulations was 0.001 ps; the electrostatic interactions were treated with the particle-mesh Ewald (PME) method with a Coulomb cutoff of 1.7 nm, Fourier spacing of 0.12 nm, and a fourth-order interpolation; the van der Waals interactions were treated using a Lennard–Jones potential and a switching function with a cutoff distance of 1.1 nm and a switching distance of 0.9 nm.

The systems equilibrated at different temperatures were used as starting models for further molecular investigations. Protein structure prediction was pursued by means of the PDBsum tool.<sup>20</sup>

**Enzymatic Hydrolysis.** LF (1 mg mL<sup>-1</sup>) was solubilized in 50 mM HEPES buffer of pH 7.2, containing 10 mM CaCl<sub>2</sub>. The protein solution was incubated for 15 min at 25 or 70 °C prior to hydrolysis. Appropriate aliquots of thermolysin solution (the enzyme solution, 2 mg mL<sup>-1</sup>, was prepared in HEPES buffer) were added to 1 mL of LF solution in order to obtain an enzyme-to-substrate molar ratio of 1:120 for digestion at 70 °C and 1:48 for digestion at 25 °C. Hydrolysis of LF was stopped by adding 2% (v/v) trifluoroacetic acid, which decreased the mixture pH to 2.0. The hydrolysates were stored at –80 °C before examination.

In order to establish the evolution of the degree of hydrolysis (DH), the enzymatic hydrolysis of LF was followed continuously for 10 min by the *o*-phthaldialdehyde (OPA) technique, as described by Church et al. (1983).<sup>21</sup> The chip-based capillary electrophoresis system (Experion, Bio-Rad) was used, both in reducing and nonreducing conditions, to analyze the extent of hydrolysis based on molecular weight (MW) distribution. Priming of the Experion Pro260 chip with gel stain and loading of the chip with gel stain, samples, and ladder were performed according to the Experion system instructions.

Electrophoresis and analysis were performed using the Experion Pro260 analysis kit protocol.

## RESULTS AND DISCUSSION

**Analysis of Thermally Induced Conformational Changes on LF at the Single-Molecule Level.** The polypeptide chain folds into two symmetrical lobes, N and C, made up of  $\alpha$ -helix and  $\beta$ -pleated sheet structures that define two domains (I and II) for each lobe. The two lobes are connected through a three-turn helix consisting on amino acids 334–344.<sup>22</sup>

The *in silico* approach was used to gather information at the atomic level on the thermal behavior of the LF molecule. The root-mean-square deviation (RMSD) obtained by least-squares fitting the LF models thermally treated at 25 and 80 °C was 2.93 Å, therefore suggesting conformational rearrangements at higher temperature. The main conformational difference between models equilibrated at 25 and 80 °C concerned the relative lobe and domain orientations: the RMSD estimated for the N- and C-lobe was 2.63 and 2.62 Å, respectively. The analysis of the two models showed that the temperature increase caused the compression of the hinge connecting the N- and C-lobes. The hinge is stabilized through 14 hydrogen bonds (Hb) at both tested temperatures. In native conformation most of the Hb is established between amino acids of the helix (the exceptions are Arg<sup>341</sup>-Gly<sup>387</sup> and Arg<sup>341</sup>-Asp<sup>390</sup>), while in the case of the protein thermally treated at 80 °C, 6 Hb involving amino acids of the C-lobe were identified. The decrease of ~6% of the total length of the Thr<sup>334</sup>-Arg<sup>344</sup> helix induced slight changes in protein structure and determined the two lobes of the protein coming closer together (Table 1).

**Table 1. Structural Indicators of LF Molecule Thermally Treated at 25 and 80 °C**

descriptors	temperature	
	25 °C	80 °C
Secondary Structure Descriptors		
strand, %	17.3 ± 0.02	16.1 ± 0.06
alfa helix, %	23.5 ± 0.15	21.2 ± 0.20
helix 3–10, %	3.8 ± 0.06	7.7 ± 0.06
Quaternary Structure Descriptors <sup>a</sup>		
$D_{NC}$ , nm	4.69 ± 0.04	4.63 ± 0.03
$L_{NC}$ , nm	1.36 ± 0.02	1.28 ± 0.02

<sup>a</sup> $D_{NC}$  is distance between the centers of mass of N- and C-lobes;  $L_{NC}$  is total length of the hinge connecting the N- and C-lobes.

Each lobe of the LF molecule has two similar anion-binding sites.<sup>19,23</sup> Because of the differences in the extent of domain closure of each lobe, the amino acids of the anion-binding site of the N-lobe, namely, Asp<sup>60</sup>, Tyr<sup>92</sup>, Tyr<sup>192</sup>, and His<sup>253</sup>, are closer together with respect to their homologues Asp<sup>395</sup>, Tyr<sup>433</sup>, Tyr<sup>526</sup>, and His<sup>595</sup> from the C-lobe (Figure 1). The distances between these amino acids were estimated based on the spatial coordinates of each atom. The effect of the thermal treatment on the LF structure can be estimated also based on the distances between the amino acids of the anion-binding sites. In the case of both N- and C-lobes, changes of the relative orientation of these amino acids were observed, as well as a general decrease of the distances between them (Figure 1).

The molecular models equilibrated at 25 and 80 °C were compared based on the structural and conformational details

obtained through the ProMotif program.<sup>20</sup> The elements of the secondary structure mainly altered by the thermal treatment are presented in Table 1. The average structural properties of LF highly depend on the temperature. Analysis of the two structures equilibrated at 25 and 80 °C indicated that a temperature increase results in the decrease of the elements of the regular secondary structure, such as strand and  $\alpha$ -helix content (Table 1).

Regardless of temperature, the secondary structure is dominated by the  $\alpha$ -helix motif (23.5% at 25 °C and 21.2% at 80 °C). Although the total number of residues involved in helix formation decreased with temperature, the number of helices increased from 28 at 25 °C to 37 at 80 °C. Some helices became shorter with increasing temperature, by losing two to four residues with respect to the native protein, whereas some amino acid sequences got a helical organization (Table 2). As a consequence of changes occurring in distances and angles between motifs, an increase of about 37% of the interacting pairs of helices in the protein occurred with increasing temperature. At 25 °C most of the helix contacts involved amino acid residues mostly internal to the helix and occasionally located beyond the C terminus of the helix. The temperature increase caused important changes in the helix interaction type. The interactions between amino acids located beyond the C and N terminus of the helix are predominant, therefore indicating a less ordered structure of the protein.

The strands within the LF structure are organized within three parallel, three antiparallel, and one mixed  $\beta$ -sheet, representing 16.1–17.3% of the protein secondary structure (Table 1). The temperature increase from 25 to 80 °C caused a decrease of the total number of strands organized as antiparallel  $\beta$ -sheets from 13 to 11. The native protein contains one  $\beta$ -hairpin motif for each lobe, consisting of two  $\beta$ -strands that are antiparallel and hydrogen bonded together. The high-temperature-dependent dynamics of hydrogen bonding affected the strand connections in such a way that lobe N lost the  $\beta$ -hairpin motif (strand 1 Tyr<sup>227</sup>-Leu<sup>230</sup> and strand 2 Arg<sup>236</sup>-Lys<sup>237</sup>). Our results comply with the observation of Sánchez et al. (1992),<sup>24</sup> who reported a higher denaturation temperature for the C-lobe of LF because of the more compact structure with respect to the N-lobe.

Some other strands of the LF structure are organized as beta–alpha–beta motifs, which are very stable with temperature increases (Table 3). The beta–alpha–beta units consist of two parallel hydrogen-bonded  $\beta$ -strands connected by a loop containing at least one  $\alpha$ -helix.

The content of the unordered structure did not change significantly with the temperature and was dominated by  $\beta$ -turn motifs. The total number of  $\beta$ -turns decreased from 109 at 25 °C to 97 at 80 °C, whereas the number of  $\gamma$ -turns increased from 7 to 11. All these molecular events are a measure of protein denaturation, which may result in loss of protein bioactivity. For example, Sui et al. (2010)<sup>10</sup> suggested that heat treatment significantly influences the iron content, depending on the degree of saturation and the intensity of the heat treatment. Heating at 72 °C for 15 s did not significantly change the free iron content (3.7%). However, treatment at 90 °C for 10 min increased the free iron content to 21% of the total iron content, suggesting a large decrease in the iron-binding ability of the native LF molecules. More severe heating conditions (90 °C for 10 min) caused a substantial increase in the free ferric iron content (27.6% of total), suggesting that



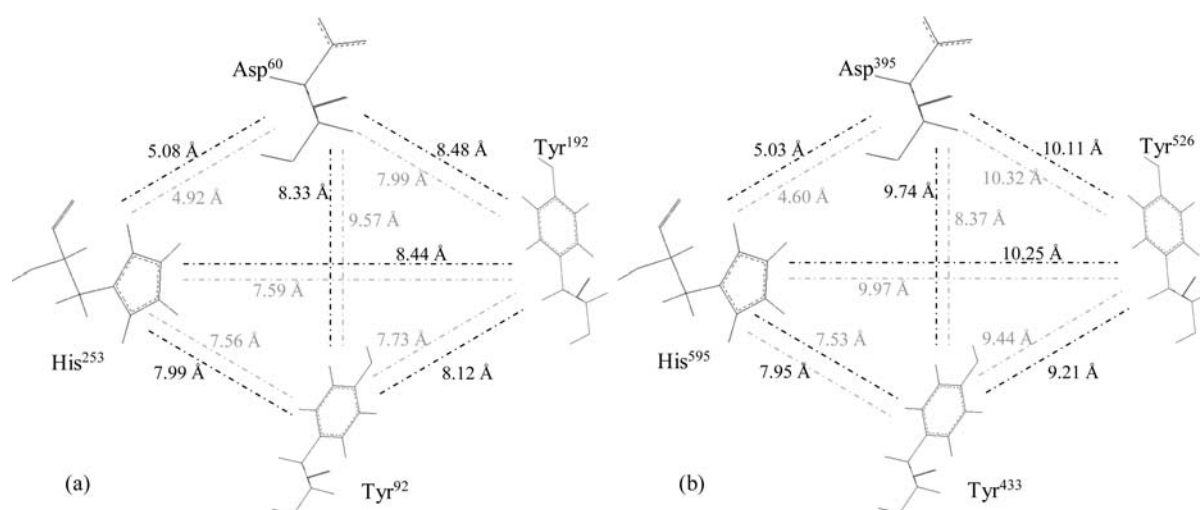


**Figure 1.** Atomic details concerning the amino acids from the N-lobe (a) and C-lobe (b) involved in iron binding. The numbers indicated on the lines represent the distances between the centers of mass of each two connected amino acids. The results characterizing the structures equilibrated at 25 and 80 °C are presented with black and light gray, respectively.

**Table 2. Influence of the Temperature Increase on the Helical Organization of the Amino Acids within the Lactoferrin Structure**

helices affected by the temperature increase	new helices formed at high temperature
Ile <sup>127</sup> -Thr <sup>131</sup> , Tyr <sup>192</sup> -Asn <sup>201</sup> , Phe <sup>242</sup> -Glu <sup>244</sup> , Glu <sup>264</sup> -Ala <sup>274</sup> , Ala <sup>322</sup> -Gln <sup>329</sup> , Ala <sup>335</sup> -Glu <sup>343</sup> , Thr <sup>377</sup> -Val <sup>384</sup> , Phe <sup>398</sup> -Lys <sup>404</sup> , and Tyr <sup>526</sup> -Ala <sup>534</sup>	Ser <sup>122</sup> -Asn <sup>126</sup> , Glu <sup>221</sup> -Arg <sup>224</sup> , Ser <sup>316</sup> -Leu <sup>320</sup> , Asn <sup>330</sup> -Arg <sup>332</sup> , Ile <sup>381</sup> -Lys <sup>386</sup> , Ala <sup>402</sup> -Cys <sup>405</sup> , Cys <sup>425</sup> -His <sup>427</sup> , Leu <sup>474</sup> -Asn <sup>476</sup> , Phe <sup>483</sup> -Lys <sup>485</sup> , Pro <sup>559</sup> -Ala <sup>561</sup> , and Leu <sup>574</sup> -Gly <sup>576</sup>

**Table 3. Atomic Details Concerning the Beta-Alpha-Beta Units within the LF Molecular Structure at 25 and 80 °C**

temperature	strand 1	strand 2	no. of helices	no. of residues	
				loop	helix
25 °C	Ser <sup>5</sup> -Thr <sup>10</sup>	Ser <sup>33</sup> -Arg <sup>38</sup>	1	22	15
	Ser <sup>114</sup> -Cys <sup>115</sup>	Ser <sup>156</sup> -Cys <sup>157</sup>	3	40	20
	Val <sup>1345</sup> -Val <sup>1350</sup>	Val <sup>1369</sup> -Ala <sup>1374</sup>	1	18	15
	Ser <sup>456</sup> -Cys <sup>457</sup>	Ser <sup>490</sup> -Cys <sup>491</sup>	1	32	6
80 °C	Val <sup>6</sup> -Thr <sup>10</sup>	Val <sup>34</sup> -Arg <sup>38</sup>	1	23	15
	Ser <sup>114</sup> -Cys <sup>115</sup>	Ser <sup>156</sup> -Cys <sup>157</sup>	2	40	14
	Val <sup>1345</sup> -Val <sup>1350</sup>	Val <sup>1369</sup> -Ala <sup>1374</sup>	1	18	16
	Ser <sup>456</sup> -Cys <sup>457</sup>	Ser <sup>490</sup> -Cys <sup>491</sup>	1	32	6

thermal treatments impaired the iron-binding ability of holo-LF molecules.<sup>10</sup>

Kawakami et al. (1992)<sup>25</sup> found a 15–30% loss of iron-binding capacity of bovine native LF after heating at 90 °C for 4 min. Similarly, Mata et al. (1998)<sup>26</sup> observed a 50% loss of iron-binding ability of human native LF in buffer after heating at 85 °C for 20 min.

**Intrinsic Fluorescence Spectroscopy.** Aromatic residues (Phe, Trp, and Tyr) contribute to hydrophobic interactions that stabilize the core because they have relatively large apolar surface areas. Additionally, they provide enhanced stability when arranged in a stacked configuration, where they not only maximize van der Waals contacts but benefit from  $\pi$ - $\pi$  interactions.<sup>18</sup> Hence, the tryptophan (Trp) residues are often found fully or partially buried in the hydrophobic core of protein interiors, at the interface between two protein domains or subdomains, or at the subunit interface in oligomeric protein

systems.<sup>16</sup> Upon disruption of the protein's tertiary or quaternary structure, these side chains become more exposed to solvent. During heating, reversible and first-order unfolding of a protein may possibly occur, through a mechanism involving partially unfolded "molten-globule" intermediate states that can result irreversibly in higher order aggregation and precipitation.<sup>27,28</sup>

The maximum emission wavelength of the intrinsic fluorescence spectrum ( $\lambda_{\max}$ ) was used to follow the structural changes of the protein induced by different temperature conditions. In the whole temperature range studied, LF had two maximum emissions around 343 and 354 nm, suggesting that the Trp residues are almost completely exposed to water, even at higher temperature. However, our results revealed that the distance between Tyr and Trp is high enough to give two emission peaks for Trp and Tyr residues. In the unfolded state, most Trp residues in proteins have a maximum emission at  $\sim$ 355 nm.<sup>12</sup>

The emission spectrum represents a highly sensitive criterion to be used for the evaluations of changes in the native state of a protein. The fluorescence emission spectra for heat-treated protein solutions are shown in Figure 2. The thermal treatment up to 80 °C induced an increase in the fluorescence intensity, evidencing the decrease of intramolecular quenching of Trp. Therefore, the fluorescence intensity of LF solutions exhibited an increase of  $\sim$ 6% after 10 min at 65 °C and about 62% when heating at 80 °C.

In order to explain these changes, a detailed analysis at the atomic level was carried out, indicating that there are 13 Trp residues in the LF structure, located in positions 8, 16, 22, 24, 125, 138, 268, 347, 361, 448, 467, 549, and 560. The emission properties of the exposed Trp residues could be influenced by surrounding amino acids that may quench its fluorescence. According to our molecular modeling experiments, the Trp fluorescence might be influenced by their Trp, Phe, and Tyr neighbors presented in Table 4.

**ANS Binding Sites.** Hydrophobic interactions are considered to play an important role in protein folding and protein stabilization. All amino acid residues with aromatic rings in their molecules are hydrophobic; therefore, Phe, Tyr, and Trp are

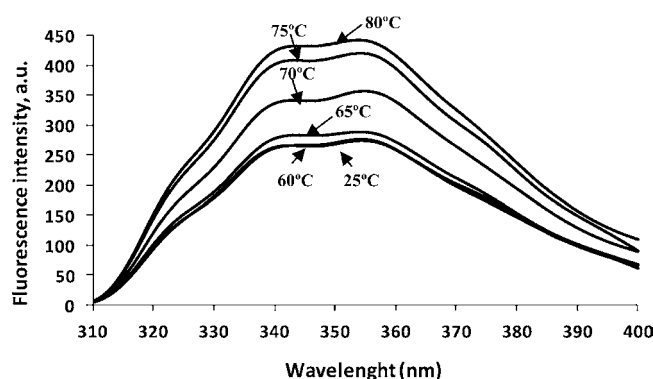


**Figure 2.** Structural changes of LF monitored by intrinsic fluorescence emission spectra at different temperatures. The excitation wavelength was 292, and the emission data were collected between 300 and 400 nm. The temperature values are indicated in the vicinity of the corresponding line. Three independent tests were carried out in each case, and SD was lower than 3.5%.

**Table 4. Atomic Details Showing the Potential Influence of Different Amino Acids on Trp Fluorescence**

pairs of amino acids	distance between amino acids (Å)	
	25 °C	80 °C
Trp <sup>347</sup> to Trp <sup>361</sup>	2.97	3.21
Trp <sup>125</sup> to Trp <sup>138</sup> , Phe <sup>43</sup> , Phe <sup>190</sup> , Phe <sup>208</sup> , Tyr <sup>92</sup> , Tyr <sup>166</sup> , Tyr <sup>192</sup> , and Tyr <sup>324</sup>	7.78, 7.04, 10.26, 10.86, 7.28, 7.11, 6.80, and 6.61	7.13, 7.32 Å, 11.26, 6.17, 7.83, 7.96, 5.56, and 7.15
Trp <sup>138</sup> to Phe <sup>152</sup> , Tyr <sup>135</sup> , and Tyr <sup>166</sup>	7.70, 6.28, and 9.55	6.40, 5.07, and 9.04
Trp <sup>268</sup> to Trp <sup>8</sup> , Phe <sup>307</sup> , and Phe <sup>686</sup>	8.90, 3.65, and 8.29	6.98, 2.78, and 9.60
Trp <sup>448</sup> to Trp <sup>467</sup> , Phe <sup>486</sup> , Phe <sup>487</sup> , and Phe <sup>542</sup>	7.53, 5.99, 7.27, and 3.26	8.03, 6.09, 7.17, and 3.96
Trp <sup>560</sup> to Phe <sup>530</sup> , Phe <sup>569</sup> , Tyr <sup>523</sup> , and Tyr <sup>526</sup>	2.73, 7.70, 6.11, and 7.85	2.46, 6.95, 9.10, and 5.82

the major constituents of hydrophobic regions<sup>29</sup> and are usually packed in the interior of the protein.

Fluorescence measurements on the LF–ANS complex give information on changes of protein–probe interactions and on the variations of the accessible hydrophobic areas. The interaction of the aromatic chromophore ANS with exposed hydrophobic clusters in a protein due to heating is accompanied by a considerable increase in the dye fluorescence intensity and a pronounced blue shift of the fluorescence maximum. Interestingly, in our ANS-binding experiments with LF at different temperatures, the maximum emission wavelength of the ANS-bound protein when excited at 365 nm remains constant around 525 nm in the whole temperature range studied. However, a small red shift in  $\lambda_{\max}$  for ANS fluorescence was observed. Two denaturation temperatures ( $T_m$ ) of 60.4 °C (for lobe N) and 89.1 °C (for lobe C) were reported in the literature for bovine LF at neutral pH.<sup>26,30,31</sup> It has been suggested that these differences are due to different heat sensitivities of the two lobes of LF, since the C-lobe appears more compact than the N lobe in the iron-saturated protein, and the presence of monoferric species.

Nevertheless, it can be seen that an increase in temperature is accompanied by significant changes in the intensity of ANS fluorescence (Figure 3), due to progressive unfolding or folding of the protein. It was observed that there is a minimal binding of ANS in the protein in its native state, which gradually increases with the temperature. This parameter reaches a

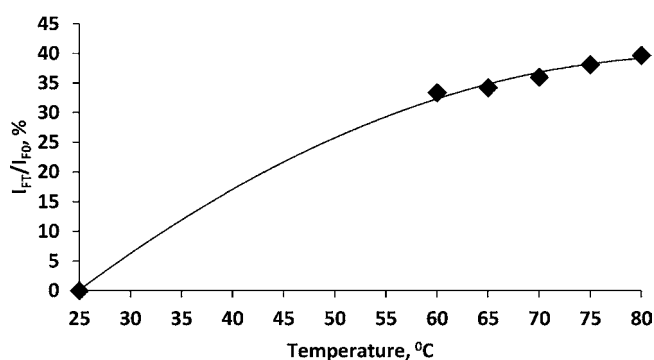


**Figure 3.** Heat-induced structural changes of LF monitored by the increase in ANS fluorescence emission, based on the  $I_F/I_{F0}$  ratio at  $\lambda_{\max}$ .  $I_{F0}$  and  $I_F$  represent the fluorescence intensity for the untreated solutions and heat-treated at temperature  $T$ , respectively. The excitation wavelength was 365, and the emission data were collected between 400 and 600 nm. All measurements were carried out in triplicates.

maximal value when heating was performed at 80 °C, suggesting the appearance of new solvent-exposed hydrophobic surfaces. Heating at this temperature caused a 1.4-fold increase in the accessible hydrophobicity, indicating that the protein was highly susceptible to thermally induced conformational changes and could possibly be in a stable, partially folded conformation under these conditions. It is important to mention that the ANS simply binds transiently to partially folded intermediates without measurably altering their conformations or stabilities and thus perturbs significantly neither the folding pathway nor its kinetics.<sup>32</sup> Our results are in good agreement with those reported by Sreedhara et al. (2010),<sup>12</sup> who compared the structural stability of bovine and caprine LF in different pH (2.0–8.0) and temperature conditions. From our results it seems that ANS binds more to a partially folded state compared to native and denatured states of the protein.

**Phase Diagram.** Native, unfolded, folded, and denatured conformations may be easily discriminated using a multi-parametric approach, because the structural properties of a protein in these conformations are very different.<sup>33</sup> Permyakov et al. (1980)<sup>34</sup> showed that such an approach is extremely sensitive to the accumulation of any intermediate state. The linear dependence of  $I_{320}$  versus  $I_{365}$  gives indications about the all-or-none transition between two different conformations.<sup>35</sup> On the other hand, the nonlinearity of this function reflects the sequential character of structural transformations.<sup>36</sup> Moreover, each linear portion will describe an individual all-or-none transition. This method was employed here to detect the existence of intermediate folding states of LF.

The fluorescence phase diagram based on intrinsic fluorescence intensity values describing the heat-induced structural changes of LF at different temperatures is given in Figure 4a. As it can be seen, it consists of a linear part corresponding to the temperature range between 25 and 80 °C. The heat treatment of globular proteins causes the destruction of some of the forces that stabilize the native conformations, such as hydrogen bonds and hydrophobic interactions. As shown in Figure 4a, the LF conformation seems to be more rigid at 60 °C and significantly more flexible at 80 °C, this statement being supported by the results outlined earlier. It can be concluded that in the whole temperature range the unfolding of the molecules is the single-phase reaction. Kussendragger (1994)<sup>37</sup> and Indyk et al. (2007)<sup>38</sup> suggested

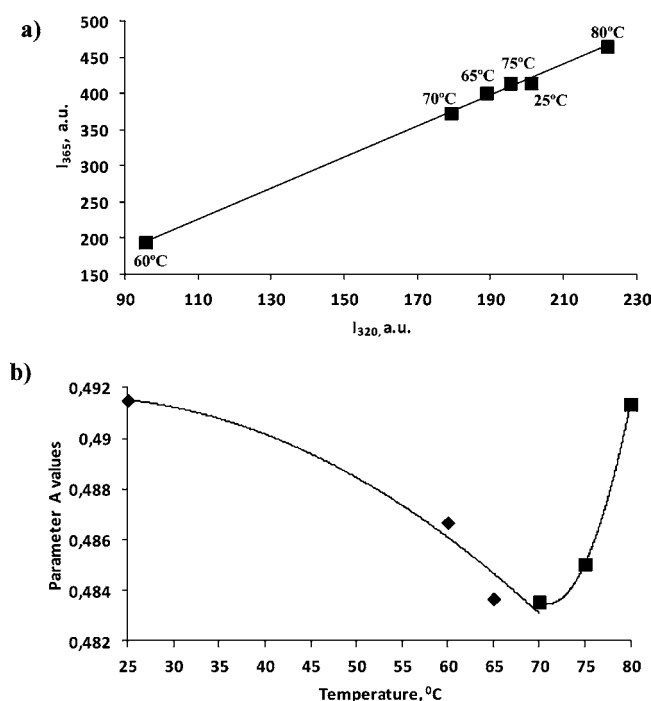


**Figure 4.** Association state of LF at different temperature values characterized by a phase diagram analysis (a) and parameter A values (b) based on intrinsic fluorescence intensity values measured at wavelengths 320 and 365 nm. For the phase diagram, the temperature values are indicated in the vicinity of the corresponding symbol. For the parameter A values: (◆) temperature range 25 to 70 °C, (■) temperature range 70 to 80 °C.

also a first-order process for LF unfolding in the temperature range 70–90 °C at neutral pH. Bengoechea et al. (2010)<sup>30</sup> highlighted that the heat treatment at 75 °C for 20 min caused an unfolding process of the lobe with the lower  $T_m$ , whereas the lobe with the higher  $T_m$  remained intact. Analyzing the results shown in Figure 4a, it can be concluded that heat treatment in the temperature range of 60 to 80 °C caused the unfolding of both lobes, with the occurrence of new intermediate molecular species.

The forces driving the protein structure are hydrophobic effects, van der Waals forces, H-bonds, and electrostatic interactions.<sup>39</sup> The protein flexibility is directly related to the interactions stabilizing the 3D structure, which are extremely complex. According to Halle (2002),<sup>40</sup> in addition to the secondary structure elements, protein flexibility is highly correlated with solvent-accessible surface. The hydrophobic contribution to the total surface of a single LF molecule was measured by means of an *in silico* approach. The hydrophobic surface available to the solvent (HSAS) was calculated as the van der Waals envelope of the proteins expanded by the radius of the solvent sphere about each solute atom center and

represents 47.9–48.3% of the total solvent-accessible surface of the LF. As a consequence of LF unfolding with increasing temperature, a slight increase of the HSAS was obtained (Table 5). The conformational rearrangements allowed the exposure of new amino acids to the explicit water molecules, whereas several other amino acids of the surface were buried. A dynamic of hydrogen bonding was therefore observed when analyzing the solvated protein model equilibrated at 25 and 80 °C. Most of the hydrogen bonds established within the protein structure or between water molecules and protein in native conformation were broken at higher temperature. The partial loss of the tertiary and secondary structure of the LF induced a decrease of approximately 5% of the hydrogen bonds stabilizing the protein backbone (Table 6). The newly yielded acceptors and donors involving surface residues partly interacted with water molecules. A slight decrease of the total number of Hb between protein and water molecules was observed at higher temperature, coupled with the increase of HSAS and of protein–water interaction energy (Table 5), which is an important component of the solvated protein total energy.

The densely packed structure of the protein is due not only to the extensive hydrogen bonding of the secondary structure elements,  $\alpha$ -helices and  $\beta$ -sheets, but also to the fact that the disulfide bridges impose supplementary connectivity constraints (Halle, 2002).<sup>40</sup> Therefore the motion of the backbone segments is limited even at high temperatures.

In the holo state the two lobes of the protein are closed and probably some of the interactive sites are buried within the interdomains. Moreover, in the iron-saturated conformation, the protein is more compact and the binding of the ferric ion contributes to maintaining the structure and disulfide bonding integrity.

The disulfide cross-links greatly contribute to the stability of the protein molecules. LF structure is stabilized through 17 disulfide bridges: Cys<sup>9</sup>-Cys<sup>45</sup>, Cys<sup>19</sup>-Cys<sup>36</sup>, Cys<sup>115</sup>-Cys<sup>198</sup>, Cys<sup>157</sup>-Cys<sup>173</sup>, Cys<sup>160</sup>-Cys<sup>183</sup>, Cys<sup>170</sup>-Cys<sup>181</sup>, Cys<sup>231</sup>-Cys<sup>245</sup>, Cys<sup>348</sup>-Cys<sup>380</sup>, Cys<sup>358</sup>-Cys<sup>371</sup>, Cys<sup>405</sup>-Cys<sup>684</sup>, Cys<sup>425</sup>-Cys<sup>647</sup>, Cys<sup>457</sup>-Cys<sup>532</sup>, Cys<sup>481</sup>-Cys<sup>675</sup>, Cys<sup>491</sup>-Cys<sup>505</sup>, Cys<sup>502</sup>-Cys<sup>515</sup>, Cys<sup>573</sup>-Cys<sup>587</sup>, and Cys<sup>625</sup>-Cys<sup>630</sup>. In native conformation, nine disulfide bridges are left-handed spiral type, while four are right-handed hook, which are known to prevail in protein structure.<sup>41</sup> The thermal treatment at 80 °C caused only slight changes in the type of disulfide cross-links; as a consequence of the rotation around some bonds in the molecule, the disulfide chain Cys<sup>502</sup>-Cys<sup>515</sup> was classified as a left-handed spiral.

The salt bridges were computed by means of VDM software using an oxygen–nitrogen cutoff distance of 3.2 Å. The number of salt bridges increases from 28 to 31 with the temperature increase from 25 to 80 °C. Only ~54% of the initial salt bridges resisted the temperature treatment at 80 °C, whereas 13 salt bridges are disrupted. At high temperature, the conformational changes in the protein are accompanied by the formation of 16

**Table 5. Molecular and Energetic Descriptors of LF under Thermal Treatment**

descriptor	temperature	
	25 °C	80 °C
total energy, kJ mol <sup>-1</sup>	-2 146 500.89 ± 1661.40	-1 800 142.02 ± 1574.41
protein–water interaction energy, kJ mol <sup>-1</sup>	-84 652.81 ± 2307.82	-84 553.72 ± 1698.69
HSAS, nm <sup>2</sup>	168.59 ± 2.45	170.85 ± 1.99
total surface, nm <sup>2</sup>	352.01 ± 2.75	353.78 ± 2.78

Table 6. Structural Indicators Concerning Hydrogen Bonding in Thermally Treated LF Molecule<sup>a</sup>

		temperature					
		25 °C			80 °C		
		MM	MS	SS	MM	MS	SS
Hb within protein	number	305	140	87	290	142	86
	length, Å	2.6–3.4	2.5–3.4	2.4–3.4	2.5–3.4	2.6–3.4	2.4–3.2
double Hb within protein	number	0	0	14	0	4	16
	length, Å			2.5–2.8		2.8–3.2	2.5–3.2
bifurcated Hb within protein	number	18	43	37	9	42	44
	length, Å	2.7–3.1	2.6–3.4	2.5–3.4	2.9–3.3	2.6–3.4	2.4–3.0
Hb water–protein	number	1301			1257		

<sup>a</sup>Hb, hydrogen bonds; MM, main chain–main chain; MS, main chain–side chain; SS, side chain–side chain.

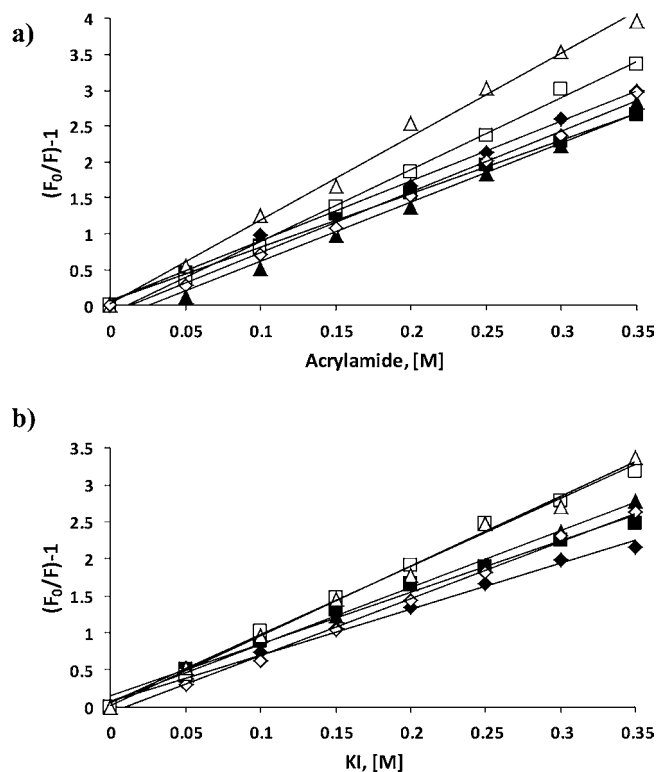
new salt bridges, mainly involving the anionic carboxylate of Asp residues.

Figure 4b indicates that, in the temperature range of 25 to 70 °C, the parameter *A* value, which characterizes the shape and position of the fluorescence spectrum, slightly decreased. Further increase of the temperature up to 80 °C led to a slight increase of the parameter *A* value to a similar value to that for the untreated solutions. Further, these results allowed detecting intermediate species (populated at 60–70 °C), responsible for the increase of ANS fluorescence intensity (Figure 3). This observation supports the importance of the multiparametric approach for the analysis of conformational transformations in proteins. Schwarcz et al. (2008)<sup>42</sup> suggested formation of soluble polymers at 70 °C involving noncovalent interactions between protein molecules, whereas the aggregates formed by heating at 80 °C dissociated under reducing conditions into monomeric LF bands, indicating that they were covalently linked.

**Acrylamide and KI Quenching Experiments.** It has been shown that the quenching of Trp residues fluorescence by different types of quenchers can provide information about the accessibility to solvent of these residues in proteins and the polarity of their microenvironment.<sup>43</sup> The approach used for carrying out the quenching experiments was previously reported.<sup>27,28</sup> Acrylamide and iodide were used as the quenchers in order to further investigate the heat-induced changes in the conformation of LF. KI is an ionic compound and can encounter and hence quench only those Trp that are exposed to the solvent. On the other hand, acrylamide can quench the fluorescence of exposed and partly buried Trp residues. The extent of quenching and hence the value of  $K_{SV}$  depend on the degree to which the quencher achieves the encounter distance of the fluorophore.

The Stern–Volmer plots for quenching of intrinsic fluorescence by acrylamide and iodide for the protein solutions heated in the temperature range 25 to 80 °C are depicted in Figure 5, a and b.

The  $K_{SV}$  values obtained with acrylamide and KI in the native state were  $7.37 \pm 0.45$  and  $6.25 \pm 0.48$  mol<sup>-1</sup> L, respectively. The maximum values were recorded at 80 °C and were 20% and ~46% higher with respect to 25 °C. LF was found to possess a much lower Stern–Volmer quenching constant than free Trp, which has a value of  $22.0 \pm 0.5$  mol<sup>-1</sup> L.<sup>44</sup> However, the lower accessibility of acrylamide to Trp residues in the native and heat-induced state compared to that of free Trp residues in water indicates that some of the residues are exposed, while some residues are located within the protein matrix. The increase of the quenching constants with the



**Figure 5.** Acrylamide (a) and KI (b) quenching of tryptophan fluorescence of heat-treated LF.  $F_0$  and  $F$  are the fluorescence intensities in the absence and presence of the quencher, respectively. The tested temperatures were (◆) 25 °C, (■) 60 °C, (▲) 65 °C, (◇) 70 °C, (□) 75 °C, (△) 80 °C.

temperature (Table 7) indicates that the conformational transition of LF brings closer together the Trp residues and

**Table 7.** Stern–Volmer Quenching Constants of Heat-Treated LF Solutions

temperature, °C	$K_{SV}$ (mol <sup>-1</sup> L)	
	acrylamide	KI
25	$7.37 \pm 0.40^a$	$6.25 \pm 0.74$
60	$7.46 \pm 0.60$	$6.99 \pm 0.88$
65	$8.26 \pm 0.64$	$7.72 \pm 0.89$
70	$8.47 \pm 0.23$	$7.74 \pm 0.65$
75	$10.00 \pm 0.45$	$9.23 \pm 0.24$
80	$11.65 \pm 0.88$	$9.39 \pm 0.47$

<sup>a</sup>Standard deviations.



quenchers. The molecular modeling tools showed that, out of the 13 Trp residues in the LF structure, only Trp<sup>268</sup>, Trp<sup>448</sup>, and Trp<sup>560</sup> are exposed to the solvent, Trp<sup>125</sup> and Trp<sup>138</sup> are partially buried, and Trp<sup>8</sup>, Trp<sup>347</sup>, Trp<sup>361</sup>, and Trp<sup>467</sup> are completely buried.

**Enzymatic Hydrolysis.** Susceptibility to enzyme hydrolysis is used as an index of flexibility since partial unfolding of protein molecules generally results in increased hydrolysis rate.<sup>45</sup> Limited proteolysis is a classical procedure to produce and isolate from relatively large globular proteins individual domains and subdomains.<sup>46</sup> The proteolysis approach was further employed to compare the susceptibility of the protein to enzymatic hydrolysis in two different states: native and partially unfolded/folded states. This approach aimed to locate the sites of initial, fast proteolysis and, consequently, the sites most flexible and prone to local unfolding, as given by the requirements of binding and adaptation at the specific stereochemistry of the active site of the protease.<sup>47,48</sup> If a protein fragment is relatively resistant to further proteolysis, it should maintain a sufficiently folded and rigid structure to prevent its extensive degradation.<sup>49</sup>

The metalloendopeptidase thermolysin (EC 3.4.24.27) was used in this study due to its thermostability up to 80 °C. The hydrolysis experiments were performed on the native and heat-induced, unfolded states of LF. The enzyme-to-substrate ratio was 1:120 at 70 °C and 1:48 at 25 °C, resulting in a relatively constant enzyme activity that was kept constant at these two temperatures.<sup>50</sup> The protein solution was heated to 70 °C for 15 min prior to addition of the enzyme, and the temperature was kept constant during hydrolysis experiments. At this temperature, the peptide bond accessibility was also investigated using bioinformatics tools and compared to that of the native protein at 25 °C.

To investigate the effects of temperature on the susceptibility of LF to proteolysis, the DH was measured during 10 min of reaction. LF was resistant to hydrolysis in both the native and heat-treated state, due to the lower substrate accessibility of the protein molecules. The initial DH obtained after 10 min of enzymatic reaction was  $0.13 \pm 0.04\%$  in the nontreated state and  $2.1 \pm 0.23\%$  for the heat-treated state, respectively. It seems that the enzymatic reaction at 70 °C resulted in structural unfolding of the protein conformation that increased the subsequent extent of proteolysis by thermolysin. These results are in agreement with the current understanding that structural changes caused by heating increase the susceptibility of the globular proteins to enzymatic hydrolysis.<sup>50</sup>

To further analyze the extent of hydrolysis, the samples further referred to as LFN (protein in its native state), LFR (LF hydrolyzed for 10 min at room temperature), and LFT (LF hydrolyzed for 10 min at 70 °C) were submitted to capillary electrophoresis analysis under both nonreducing and reducing conditions to characterize the nature of the intermolecular links involved in the aggregation of the different intermediaries of LF.

Under nonreducing conditions (Figure 6a), a single major peak with a molecular weight around 95 kDa was found for LFN, which corresponded to the monomeric form of the protein. For LFR samples, a progressive drop in the intensity of the monomeric protein peak occurred, from ~89% to 67%, with the appearance of two molecular species of about 72 kDa (~15%) and 103 kDa (~9%). The protein molecules became significantly flexible when hydrolysis experiments were performed at 70 °C. The monomer concentration decreased from 89% to ~20%, with the appearance of new molecular

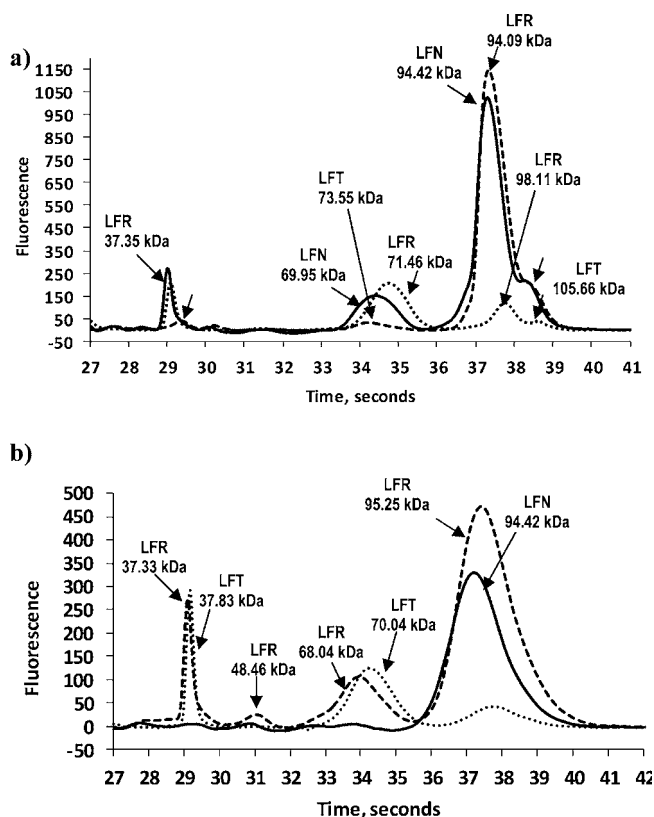


**Figure 6.** Overlays of electrophoretograms of LFN (solid lines), LFR (dashed lines), and LFT (dotted lines) in nonreducing (a) and reducing (b) conditions.

species, resulting from enzymatic hydrolysis (~55% peptides with a higher MW of 74 kDa, 5% peptides with a MW of ~28 kDa, and 18% with a MW of 38 kDa). A small proportion of protein aggregates (3.3%) with a MW of ~105 kDa appeared as well, probably as a consequence of the covalent bonding of LF monomers and peptides.

Figure 6b shows the particle size distribution of samples obtained under reducing conditions. After incubation of unheated solutions at room temperature with thermolysin, the LF peak decreased from 96% to ~74%, and new peaks corresponding to 68 kDa (14.3%) and ~38 kDa (10%) were seen. It seems that LF is quite resistant to proteolysis in its native state.

The heated solutions showed different electrophoresis patterns when compared to the unheated solutions, having two peaks, at about 36 kDa (46%) and ~38 kDa (53%). These differences suggest a higher extent of hydrolysis in the heated samples. No residual LF in solution after the incubation with thermolysin could be identified. However, analyzing the kinetics of enzymatic hydrolysis considering only a simple mechanism involving a single substrate reaction is not suitable. It is possible to have as many substrates as there are susceptible peptide bonds in proteins. The enzyme attack patterns follow several theories including random, ordered, or ping-pong sequences of peptide bond attack.<sup>51</sup>

In order to provide a more complete description, the PeptideCutter tool on the ExPASy Server<sup>52</sup> was used to predict the cleavage sites on the LF molecule. According to Keil (1992),<sup>53</sup> thermolysin preferentially cleaves the peptide bond involving bulky or aromatic residues (Ile, Leu, Val, Ala, Met, Phe) at the C-side; hydrolysis is favored when an aromatic



amino acid is located at the N-side of the peptide bond and is hindered when an acidic residue is in the same position. On the basis of the FASTA sequence, a total of 196 potential cleavage sites were identified, out of which three are located on the three-turn helix connecting the N- and C-lobes. The further detailed analysis of the 3D structure of the LF molecule allowed considering that about half of the cleavage sites located on each lobe (49 out of 96/97 in the case of the N-/C-lobe) are completely buried in the native protein and was not accessible to thermolysin. The thermal treatment at 70 °C induces conformational changes that allow a better exposure of the partially buried amino acids from the LF structure, therefore allowing a more advanced hydrolysis of the substrate.

Depending on the hydrolysis conditions, it is possible that thermolysin attack prefers the native protein, the unfolded state, or even some resulting polypeptides or even aggregates. Cheison et al. (2010),<sup>54</sup> using MALDI-TOF/MS analysis of hydrolysates of  $\beta$ -lactoglobulin, showed that at >40 °C the action of trypsin favored depletion of the native substrate first; at lower temperatures, the enzyme attacked the resulting peptides even when there was some residual protein detectable. This reaction sequence explains the apparent disparity between the DH values and protein depletion, where elevated DH values, even where some protein was detectable, suggest further breakdown of the peptides in preference to the native proteins.

Our experiments revealed that higher temperature facilitates the enzymatic hydrolysis, but it may affect the nutrition. The heat treatment at 70 °C ensures proper protein solubility in buffer solution but also an improvement in susceptibility to enzymatic hydrolysis. However, further studies are needed to fully characterize the resulting peptides and/or aggregates.

In conclusion, the molecular behavior of LF under different thermal conditions was studied using combined experimental and *in silico* approaches. The fluorescence spectroscopic methods showed that increasing the temperature over 60 °C results in an increased degree of Trp residue exposure, indicating conformational changes that favor the enzymatic hydrolysis by thermolysin.

Molecular modeling provides a powerful technique to examine at the atomic level the molecular structure of proteins and to investigate their thermal-dependent behavior. The main conformational difference between models equilibrated at 25 and 80 °C concerned the relative lobe and domain orientations. The temperature increase resulted in the decrease of the elements of regular secondary structure, such as strand and  $\alpha$ -helix content.

It is well known that heat treatment of milk and milk protein solutions affects the functional properties of native proteins. The heat stability of LF is very important for its use as a bioactive component in foods. By unifying these aspects of protein structure at the atomic level with the knowledge provided by fluorescence spectroscopic measurements, the present study contributes to a better understanding of the physical properties of LF, in terms of its use in various applications.

## AUTHOR INFORMATION

### Corresponding Author

\*Phone: +40 336 130 18. Fax: +40 236 461 353. E-mail: Iuliana.Aprodu@ugal.ro.

### Funding

N.S. and I.A. have benefited from financial support through the 2010 POSDRU/89/1.5/S/52432 project, *Organizing the na-*

*tional interest postdoctoral school of applied biotechnologies with impact on Romanian bioeconomy*, a project co-financed by the European Social Fund through the Sectoral Operational Programme Human Resources Development 2007–2013.

### Notes

The authors declare no competing financial interest.

## REFERENCES

- (1) Guo, M.; Zhang, L. Y.; Lü, W. J.; Cao, H. R. Analysis of the spectroscopic characteristics on the binding interaction between tosylloxacin and bovine lactoferrin. *J. Lumin.* **2011**, *131*, 768–775.
- (2) Spik, G.; Coddeville, B.; Montreuil, J. Comparative study of the primary structures of sero-, lacto- and ovotransferrin glycans from different species. *Biochimie* **1988**, *70*, 1459–1469.
- (3) Nisar, S.; Kazmi, S. A. Spectrofluorometric study of iron removal from bovine lactoferrin by ethylenediaminetetraacetic acid. *Spectrochim. Acta Part A: Mol. Biomol. Spectrosc.* **2010**, *77*, 933–937.
- (4) Baker, E. N. Structure and reactivity of transferrins. *Adv. Inorg. Chem.* **1994**, *41*, 389–463.
- (5) Steijns, J. M.; van Hooijdonk, A. C. M. Occurrence, structure, biochemical properties and technological characteristics of lactoferrin. *Br. J. Nutr.* **2000**, *84* (Suppl. 1), S11–S17.
- (6) Brock, J. H. The physiology of lactoferrin. *Biochem. Cell Biol.* **2002**, *80*, 1–6.
- (7) Wakabayashi, H.; Takase, M.; Tomita, M. Lactoferricin derived from milk protein lactoferrin. *Curr. Pharm. Design* **2003**, *9*, 1277–1287.
- (8) Van der Kraan, M. I. A.; Groenink, J.; Nazmi, K.; Veerman, E. C. I.; Bolscher, J. G. M.; Nieuw Amerongen, A. V. Lactoferrampin: A novel antimicrobial peptide in the N1-domain of bovine lactoferrin. *Peptides* **2004**, *25*, 177–183.
- (9) Fox, P. F.; Kelly, A. L. Developments in the chemistry and technology of milk proteins. Minor milk proteins. *Food Australia* **2003**, *55*, 231–234.
- (10) Sui, Q.; Roginski, H.; Williams, R. P. W.; Versteeg, C.; Wan, J. Effect of pulsed electric field and thermal treatment on the physicochemical properties of lactoferrin with different iron saturation levels. *Int. Dairy J.* **2010**, *20*, 707–714.
- (11) Abe, H.; Saito, H.; Miyakawa, H.; Tamura, Y.; Shimamura, S.; Nagao, E.; et al. Heat stability of bovine lactoferrin at acidic pH. *J. Dairy Sci.* **1991**, *74*, 65–71.
- (12) Sreedhara, A.; Flengsrud, R.; Prakash, V.; Krowarsch, D.; Langsrud, T.; Kaul, P.; Devold, T. G.; Vegarud, G. E. A comparison of effects of pH on the thermal stability and conformation of caprine and bovine lactoferrin. *Int. Dairy J.* **2010**, *20*, 487–494.
- (13) Polverino de Laureto, P.; Scaramella, E.; Frigo, M.; Geffer Wondrich, F.; De Filippis, V.; Zamboni, M.; Fontana, A. Limited proteolysis of bovine  $\alpha$ -lactalbumin: Isolation and characterization of protein domains. *Protein Sci.* **1999**, *8*, 2290–2303.
- (14) Dodson, G. G.; Lane, D. P.; Verma, C. S. Molecular simulations of protein dynamics: New windows on mechanisms in biology. *EMBO Rep.* **2008**, *9*, 144–150.
- (15) Van Gunsteren, W. F.; Dolenc, J.; Mark, A. E. Molecular simulation as an aid to experimentalists. *Curr. Opin. Struct. Biol.* **2008**, *18*, 149–153.
- (16) Royer, C. A. Probing protein folding and conformational transitions with fluorescence. *Chem. Rev.* **2006**, *106*, 1769–1784.
- (17) Bushmarina, N. A.; Kuznetsova, I. M.; Biktashev, A. G.; Turoverov, K. K.; Uversky, V. N. Partially folded conformations in the folding pathway of bovine carbonic anhydrase II: A fluorescence spectroscopic analysis. *ChemBioChem* **2001**, *2*, 813–821.
- (18) Kuznetsova, M.; Turoverov, K. K.; Uversky, V. N. Use of the phase diagram method to analyze the protein unfolding-refolding reactions: Fishing out the “invisible” intermediates. *J. Proteome Res.* **2004**, *3*, 485–494.
- (19) Moore, S. A.; Anderson, B. F.; Groom, C. R.; Haridas, M.; Baker, E. N. Three-dimensional structure of diferric bovine lactoferrin at 2.8 Å resolution. *J. Mol. Biol.* **1997**, *274*, 222–236.

- (20) Laskowski, R. A. PDBsum new things. *Nucleic Acids Res.* **2009**, *37*, D355–D359.
- (21) Church, F. C.; Swaisgood, H. E.; Porter, D. H.; Catignani, G. L. Spectrophotometric assay using *o*-phthalaldehyde for determination of proteolysis in milk and isolated milk proteins. *J. Dairy Sci.* **1983**, *66*, 1219–1227.
- (22) González-Chávez, S. A.; Arévalo-Gallegos, S.; Rascón-Cruz, Q. Lactoferrin: Structure, function and applications. *Int. J. Antimicrob. Agents* **2009**, *33*, 301.e1–301.e8.
- (23) Williams, R.; Sui, Q.; Roginski, H.; Wooster, T.; Versteeg, C.; Wan, J. Effect of ionic strength of pulsed electric field treatment medium on the physicochemical and structural characteristics of lactoferrin. *J. Agric. Food Chem.* **2010**, *58*, 11725–11731.
- (24) Sánchez, L.; Peiró, J. M.; Castillo, H.; Pérez, M. D.; Ena, J. M.; Calvo, M. Kinetic Parameters for Denaturation of Bovine Milk Lactoferrin. *J. Food Sci.* **1992**, *57*, 873–879.
- (25) Kawakami, H.; Tanaka, M.; Tatsumi, K.; Dosako, S. Effects of ionic strength and pH on the thermostability of lactoferrin. *Int. Dairy J.* **1992**, *2*, 287–298.
- (26) Mata, L.; Sánchez, L.; Headon, D.; Calvo, M. Thermal denaturation of human lactoferrin and its effect on the ability to bind iron. *J. Agric. Food Chem.* **1998**, *46*, 3964–3970.
- (27) Stănciuc, N.; Râpeanu, G.; Bahrim, G.; Aprodu, I. pH and heat-induced structural changes of bovine apo- $\alpha$ -lactalbumin. *Food Chem.* **2012**, *131*, 956–963.
- (28) Stănciuc, N.; Aprodu, I.; Râpeanu, G.; Bahrim, G. Fluorescence spectroscopy and molecular modeling investigations on the thermally induced structural changes of bovine  $\beta$ -lactoglobulin. *Innovative Food Sci. Emerging Technol.* **2012**, *15*, 50–56.
- (29) Nosoh, Y.; Sekiguchi, T. *Protein Stability and Stabilization through Protein Engineering*; Ellis Harwood: New York, 1991.
- (30) Bengoechea, C.; Peinado, I.; McClements, D. J. Formation of protein nanoparticles by controlled heat treatment of lactoferrin: Factors affecting particle characteristics. *Food Hydrocolloids* **2011**, *25*, 1354–1360.
- (31) Paulsson, M. A.; Svensson, U.; Kishore, A. R.; Naidu, A. S. Thermal behavior of bovine lactoferrin in water and its relation to bacterial interaction and antibacterial activity. *J. Dairy Sci.* **1993**, *76*, 3711–3720.
- (32) Engelhard, M.; Evans, P. H. Kinetics of interaction of partially folded proteins with a hydrophobic dye: Evidence that molten globule character is maximal in early folding intermediates. *Protein Sci.* **1995**, *4*, 1553–1562.
- (33) Uversky, V. N. Natively unfolded proteins: A point where biology waits for physics. *Protein Sci.* **2002**, *11*, 739–756.
- (34) Permyakov, E. A.; Yarmolenko, V. V.; Emelyanenko, V. I.; Burstein, E. A.; Gerday, C.; Closset, J. Fluorescence Studies of the Calcium Binding to Whiting (*Gadus merlangus*) Parvalbumin. *Eur. J. Biochem.* **1980**, *109*, 307–315.
- (35) Yang, F., Jr.; Zhang, M.; Zhou, B. R.; Chen, J.; Liang, Y. Structural changes of  $\alpha$ -lactalbumin induced by low pH and oleic acid. *Biochem. Biophys. Acta* **2006**, *1764*, 1389–1396.
- (36) Jiao, M.; Zhou, Y. L.; Li, H. T.; Zhang, D. L.; Chen, J.; Liang, Y. Structural and functional alterations of two multidomain oxidoreductases induced by guanidine hydrochloride. *Biochem. Biophys. Acta* **2010**, *42*, 30–38.
- (37) Kussendrager, K. D. Effects of heat treatment on structure and iron-binding capacity of bovine lactoferrin. In *IDF Bulletin: Indigenous Antimicrobial Agents of Milk: Recent Developments*; Brussels, Belgium, 1994; S.I. 9404, pp 133–146.
- (38) Indyk, H. E.; McGrail, I. J.; Watene, G. A.; Filonzi, E. L. Optical biosensor analysis of the heat denaturation of bovine lactoferrin. *Food Chem.* **2007**, *101*, 838–844.
- (39) Laurence, L. S.; Middaugh, C. R. Fundamental structures and behaviors of proteins. In *Aggregation of Therapeutic Proteins*; Wnag, W., Roberts, C. J., Eds.; John Wiley & Sons, Inc.: Hoboken, NJ, p 14.
- (40) Halle, B. Flexibility and packing in proteins. *Proc. Natl. Acad. Sci. U.S.A.* **2002**, *99*, 1274–1279.
- (41) Richardson, J. S. The anatomy and taxonomy of protein structure. *Adv. Protein Chem.* **1981**, *34*, 167–339.
- (42) Schwarcz, W. D.; Carnelocce, L.; Silva, J. L.; Oliveira, A. C.; Gonçalves, R. B. Conformational changes in bovine lactoferrin induced by slow or fast temperature increases. *Biol. Chem.* **2008**, *389*, 1137–1142.
- (43) Pawar, S. A.; Deshpande, V. V. Characterization of acid-induced unfolding intermediates of glucose/xylose isomerase. *Eur. J. Biochem.* **2000**, *267*, 6331–6338.
- (44) Chadborn, N.; Bryant, J.; Bain, A. J.; O'Shea, P. Ligand-dependent conformational equilibria of serum albumin revealed by tryptophan fluorescence quenching. *Biophys. J.* **1999**, *76*, 2198–2207.
- (45) Guo, M. R.; Fox, P. F.; Flynn, A.; Kindstedt, P. S. Susceptibility of  $\beta$ -lactoglobulin and sodium caseinate to proteolysis by pepsin and trypsin. *J. Dairy Sci.* **1995**, *78*, 2336–2344.
- (46) Wu, L. C.; Grandori, R.; Carey, J. Autonomous subdomains in protein folding. *Protein Sci.* **1994**, *3*, 369–371.
- (47) Fontana, A.; Polverino de Laureto, P.; De Filippis, V.; Scaramella, E.; Zamboni, M. Limited proteolysis in the study of protein conformation. In *Proteolytic Enzymes: Tools and Targets*; Sterchi, E. E., Stöcker, W., Eds.; Springer: Heidelberg, Germany, 1999; pp 253–280.
- (48) Hubbard, S. J. The structural aspects of limited proteolysis of native proteins. *Biochem. Biophys. Acta.* **1998**, *1382*, 191–206.
- (49) Nik, A. M.; Wright, A. J.; Corredig, M. Surface adsorption alters the susceptibility of whey proteins to pepsin-digestion. *J. Colloid Interface Sci.* **2010**, *344*, 372–381.
- (50) N'Negue, M.-A.; Miclo, L.; Girardet, J.-M.; Campagna, S.; Molle, D.; Gaillard, J.-L. Proteolysis of bovine  $\alpha$ -lactalbumin by thermolysin during thermal denaturation. *Inter. Dairy J.* **2006**, *16*, 1157–1167.
- (51) Garrett, R.; Grisham, C. M. *Biochemistry*, 2<sup>nd</sup> ed.; Thomson Brooks/Cole: Belmont, CA, USA, 2007; p 1100.
- (52) Gasteiger, E.; Hoogland, C.; Gattiker, A.; Duvaud, S.; Wilkins, M. R.; Appel, R. D.; Bairoch, A. Protein Identification and Analysis Tools on the ExPASy Server. In *The Proteomics Protocols Handbook*; Walker, J. M., Ed.; Humana Press: Totowa, NJ, 2005; pp 571–607.
- (53) Keil, B. *Specificity of Proteolysis*; Springer-Verlag: New York, 1992; p 335.
- (54) Cheison, S. C.; Schmitt, M.; Leeb, E.; Letzel, T.; Kulozik, U. Influence of the temperature and the degree of hydrolysis on the peptide composition of trypsin hydrolysates of  $\beta$ -lactoglobulin: analysis by LC-ESI-TOF/MS. *Food Chem.* **2010**, *121*, 457–467.